Isotope-selective radiography and material assay using high-brilliance, quasi-monochromatic, high-energy photons

M. Jentschel,[1] F. Albert,[2] T. Buslaps,[3] U. Gayer,[4] J. Hall,[2] V. Honkimaki,[3]
L. Mertes,[4] A.J. Pollitt,[1] P. Mutti,[1] N. Pietralla,[4] and C.P.J. Barty[2]

[1]*Institut Laue-Langevin, 71 Avenue des Martyrs, CS 20156, F - 38042 Grenoble Cedex 9, France*
[2]*Lawrence Livermore National Laboratory, Livermore, California 94550, USA*
[3]*European Synchrotron Radiation Facility, 71 Avenue des Martyrs, CS40220, 38043 Grenoble Cedex 9, France*
[4]*Institut fur Kernphysik, Technische Universität Darmstadt, D-64289 Darmstadt, Germany*

(Dated: October 15, 2015)

We demonstrate the possibility to perform high-fidelity, isotope selective radiography using a quasi-monochromatic high-energy photon beam. The isotope detection is based on a witness scatterer absorbing and re-emitting photons via nuclear resonance fluorescence (NRF). This enables the detection of a specific isotope with micro-gram accuracy at large distance from the actual sample. Further, we demonstrate that the technique is capable of delivering quantitative information without specific knowledge of the photon flux or the resonance fluorescence cross section. The detection of light isotopes screened by heavy shielding is also shown. The techniques described are applicable to next-generation, ultrahigh brilliance, laser-Compton light sources currently under construction.

PACS numbers: 24.30.Gd, 25.20.Dc, 07.85.Qe, 41.50.+h

The availability of a tunable quasi-mono-energetic γ-ray source enables the dedicated excitation of specific nuclear resonance levels and to observe the subsequent Nuclear Resonance Fluorescence (NRF) as an isotope specific signal [1]. NRF offers several advantages over X-ray fluorescence based techniques: The higher penetration power allows the investigation of more massive samples and those obscured by shielding. The radiation damage per unit volume is relatively small making the technique interesting for biological and medical applications. Since for a given photon energy the NRF-reaction is isotope as opposed to element dependent, it opens up new possibilities for contrast techniques in medical imaging or nuclear waste assay independent of chemical constraints. Some NRF-techniques have been realized using Bremsstrahlung sources [2], which deliver a continuous (white) γ-ray spectrum with a maximum cut off energy. Although these sources are capable of delivering substantial photon fluxes their polychromatic spectrum is not well matched to the narrow resonances typical of NRF reactions. Polychromatic output causes the majority of photons to be Rayleigh- or Compton-scattered, which deteriorates the signal to noise ratio in the detectors and consequently the sensitivity of the experiment. Sources with bandwidths of order $\Delta E/E \sim 10\%$ based on laser-Compton scattering from relativistic electrons like NewSUBARU [3], HiγS [4] and T-REX [5, 6] have been created. Some of these sources have been used to detect the presence of shielded isotopic material [7, 8]. These simple detection experiments while motivational, took hours to complete and have lacked the photon flux, required bandwidth and appropriate detector architectures for precision assay or imaging. Presently a new generation of tunable quasi-monochromatic γ-ray sources such as MEGa-ray [9], ELI-NP [10–12] or at JAEA KEK [13] are planned or already under construction with goals of producing gamma-ray fluxes 3 to 6 orders of magnitude beyond the present state of the art. These sources, based on optimized laser-Compton back scattering of high average current relativistic electron bunches and intense laser pulses, may deliver very intense photon pulses tunable from 0.1 to 20 MeV with total rate of 10^{10} ph. s^1 within a band width of order $\Delta E/E \simeq 10^{-3}$ [10]. Assuming a nuclear resonance width of 1 eV (Doppler broadened due to thermal movement) this would produce up to 10^7 ph. s^1 available for NRF excitation. A notable property of these next-generation photon sources is the pulse structure firing within a millisecond up to 10^{10} photons at the sample, a large fraction of which is scattering into the detectors.This may lead to saturation and loss of spectroscopic capabilities. The development of new detection schemes and/or the definition of suitable beam characteristics during which NRF-based techniques can be applied is required. This paper outlines a witness material based detection architecture enabling next-generation, high-flux laser-Compton machines to be routinely used for isotope-specific material detection, assay and imaging even in the presence of considerable shielding.

Of particular importance is the monochromatisation since this strongly impacts the ratio of NRF-usable photons (signal) to diffusely scattered noise. The present paper uses the NRF-reaction of ^{7}Li, which is known to occur at 477.629 keV [14], as a suitable test case to demonstrate the potential capabilities of these new experimental techniques. Additionally, Lithium is a technologically relevant element in many power systems and the development of a photon based, non-destructive, isotope sensitive detection technique for this element could contribute to the study of a number of problems in optimizing high capacity batteries. Since photon output at energies above 100 keV requires special beam and magnet configurations at synchrotrons, the only available facility

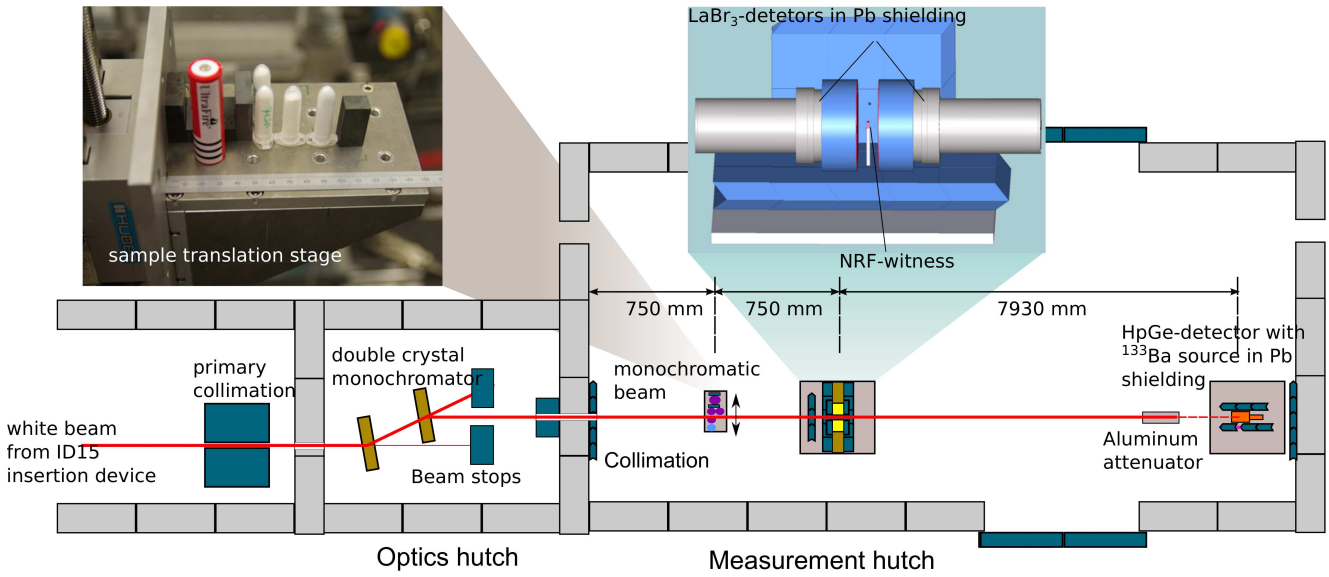

FIG. 1: Schematic Layout of the experiment at the ID15a beamline of the ESRF. The white beam from the AMPW is collimated and monochromatized in dedicated optics hutch before it passes into the measurement hutch. The prepared beam is seen by the sample, probed by the NRF-witness sample while the beam energy and intensity are monitored by a HpGe detector.

with an dedicated beam line above 100 keV is ID15a [15] at the European Synchrotron Radiation Facility (ESRF) in Grenoble, France.

At the ^{7}Li resonance of 478 keV ID15a provides a flux and average brilliance many orders of magnitude beyond previous laser-Compton-based experiments but on par with or a couple of orders of magnitude below that of next generation laser-Compton machines. We note that above 700 keV intensity at synchrotrons falls precipitously, while next-generation, laser-Compton machines provide more than 8 orders of magnitude higher intensity.

The insertion device of ID15a generates a white spectrum up to 700 keV, which passes through a water cooled low energy filter made from SiC (see Fig. 1). Further downstream the beam is shaped by a 60 mm long water cooled WC collimation system creating a rectangular beam profile (accuracy $\simeq$ 10 μm). The collimation is followed by a double bent crystal monochromator, using the [311]-plane of Germanium for diffraction in non-dispersive geometry. The first crystal is water cooled to minimize heating effects. The radius of curvature is adapted to the divergence of the beam (about 16 μradian). The monochromator geometry keeps the position of the beam constant for all energies. The beam brilliance at about 480 keV, is of the order 10^{13} ph sr^{-1} s^{-1} mm^2 at 0.1%BW. During the present experiment we used a beam cross section of 0.1×0.1 mm^2 reducing the photon flux by a factor 100 and yielding approximately 10 to 100 ph eV^{-1} s^{-1} onto the sample. This represents a substantial increase in NRF sensitive photons compared to previously used sources [5], but is still substantially below the expect flux of 10^7 ph eV^{-1} s^{-1} of future sources.

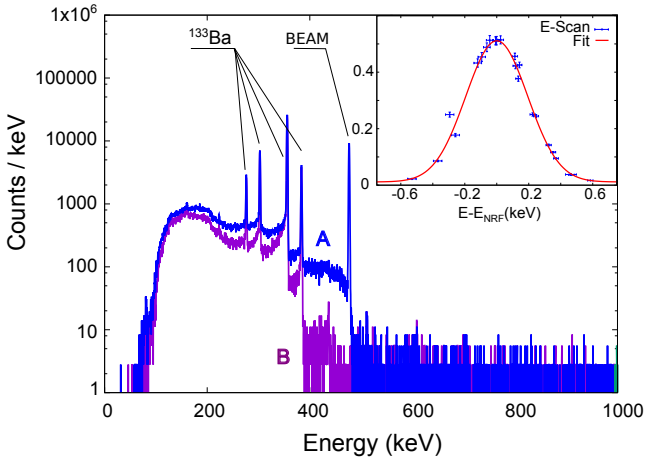

FIG. 2: Measured photon spectrum of the ID15a beam at the ESRF. The main plot shows three spectra: A) A spectrum of the ID15A beam through a 30 cm Al attenuator an additional 20 mm Pb attanuator to avoid pile-up and B) a spectrum with the ID15a beam off. The calibration sources were permanently included in the Pb shielding of the Ge-detector. The insert shows the intensity of the witness sample monitored by the $LaBr_3$ detectors as function of monochromator energy. This measurement represents a kind of high resolution scan of the monochromator response function.

The entire beam preparation is done in a dedicated optics hutch to avoid diffuse scattering into the actual measurement zone.

A remote-controlled sample table with the object to be investigated via NRF is followed downstream by a witness sample consisting of a $20 \times 10 \times 5$ mm^3 piece of natural Li metal. The witness sample was placed between

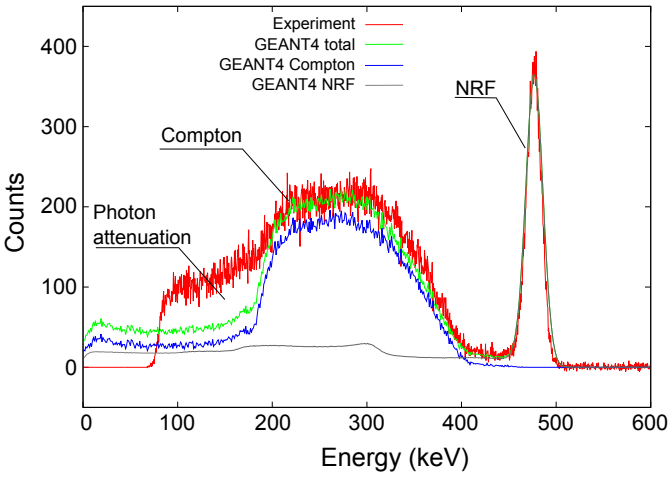

FIG. 3: Comparison of GEANT4 simulations of the witness sample setup to the experimental spectra taken with the $LaBr_3$(Ce)-detectors. A good qualitative agreement for the NRF peak and the Compton shape could be obtained. In the energy range of 100 - 200 keV the simulation does not reproduce the experiment well because the optical photon transport physics was not included in GEANT4 physics processes.

two 3 inch $LaBr_3$(Ce) detectors separated by 22 mm. The scintillating head of the detectors was enclosed in an Aluminum housing, surrounded by a 1 mm thick Cu housing followed by a lead shielding. The lead shielding was 30 mm thick in radial direction, while 1 mm was used on the front face of the detectors. Further downstream the beam passed through a 30 cm Aluminum attenuator before impinging upon a lead shielded coaxial HpGe-detector with 60% relative efficiency. A ^{133}Ba source was put inside the lead shielding of the Ge-detector to provide permanent energy and efficiency monitoring of the Ge-detector. This allowed for correction of energy and intensity drifts of the ID15A beam. Since ID15a is primarily used for experiments at energies below 100 keV, its performance at high energy in terms of energy and intensity selectivity and stability are not optimal. Beam parameter variations originated from changes of the electron current in the synchrotron storage ring, temperature related variations of the lattice spacing of the monochromator as well as angular drifts of the monochromator goniometers. Most drifts could be partially corrected during data processing using the information obtained from the Ge-detector beam monitor. However, it is worth noting that for all presented results the time instability of the beam parameters represent the main limitation.

A Ge-detector measurement of the ID15a-spectrum is shown in Fig. 2 as (A). The spectrum contains the desired peak (marked as BEAM) at 477.629 keV and the ^{133}Ba calibration lines. More detailed information on the spectral width in the vicinity of the NRF-energy can be obtained by scanning the energy settings of the monochromator and observing resonance rate of the NRF-witness sample with the $LaBr_3$(Ce) scintillators. In fact, the detected intensity profile is given by a convolution of two curves: $I_D(E) = I_M(E) * I_{NRF}(E)$, where $I_M(E)$ is the monochromator spectrum and $I_{NRF}(E)$ is the nuclear resonance profile. Since the width of the nuclear resonance is in the order of one eV, centered around E_{NRF}, its contribution to the total width can be neglected. The energy scan is shown as insert in Fig. 2 and fitted with a Gaussian yielding a spectral width of $FWHM = 0.456(4)$ keV. The transfer function of a double bent monochromator suggests a more triangular shape than a Gaussian. However, it seems that at high energies lattice deformations of the monochromator crystals become important and lead to a smoother line shape. To our knowledge this represents the first direct measurement of the response function of the monochromator at these high photon energies.

Knowing the beam characteristics and the setup geometry, the detection capability of the NRF-witness system was simulated with GEANT4 and compared to experimental data. The experimental data were obtained by subtracting the natural self-background produced by the $LaBr_3$ detectors. Due to their substantial volume it contributes up to 10% to the low energy portion of the spectrum. Since GEANT4 does not include all NRF reactions, the simulations were carried out in two stages: The first simulation calculated the Compton scattering of the ID15a beam on the witness sample and the detection of these photons. In a second, separate stage the emission and detection of the NRF signal from the withness sample was simulated. The intensity ratio of both simulations stages was fitted to match the experimental data in Fig. 3. The comparison of simulation and experiment shows a good reproduction of the high energy part (above 200 keV) of the Compton scattered spectrum. For lower energies we see a substantial deviation of the simulation from experiment. The low energy (E < 100 keV) cut-off in intensity originates from the cut-off of the self-trigger of the acquisition system. The higher intensity of experimental data in the energy range of 100 - 200 keV can be explained by the fact that optical photon transport was not included into the GEANT4 simulation to save computing time. The attenuation of 85% of γ-rays occurs dominantly within the first 4 cm of the scintillator. This leavs at least 4 cm of path length for the optical photons to reach the photo cathode. Since the attenuation length of $LaBr_3$ is about 12 cm [16] for the for $\lambda = 380$ nm scintillation light about 36% of optical photons are self-absorbed. This is equivalent to an incomplete energy signal leading to an "artificial" decrease of the lower energy spectrum. This indicates that the size of the available $LaBr_3$ detectors was not optimal for the given experiment.

Sensitive detection of Li is demonstrated by moving a pure Li-metal foil of 2.72 mm thickness in and out of the beam. To separate NRF from Compton and Raleigh scattering signals each measurement (Li metal in/out) was carried out at two beam line photon energies $E = E_{NRF}$ and $E = E_{NRF} - 2$keV. The results of all four measure-

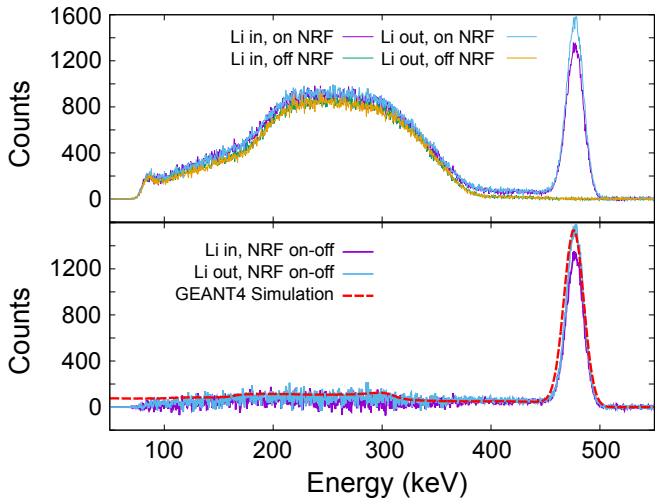

FIG. 4: Plot of four scans with Li-metal in/out and on/off NRF-energy tuning of the beam (upper part). Subtracting the off NRF-energy spectra gives pure NRF-signals for the Li in/out of beam (lower part). The Li-out beam spectrum is compared to the GEANT4 simulation of Fig. 3 showing rather good agreement and validating the subtraction approach.

ments are illustrated in Fig. 4. The on-NRF spectra can be evaluated using the classical spectroscopic approach by fitting the NRF peak and looking at the variation of peak area. The NRF-peak was attanuated by a factor of 0.88(2) by the insertion of the Li metal. The Compton scattered part of the spectrum can be removed by subtracting on and off resonant data. This approach is validated by the GEANT4 simulation of the pure NRF-emission. The newly obtained spectra can be further evaluated in two ways: i) the classical spectroscopic approach considering NRF-peak area attenuation yielding a factor of 0.86(2). ii) Since background subtraction removed all non-NRF related phenomena the integral spectrum can be used for calculating an attenuation factor. This approach yield an attenuation factor of 0.82(1). In all three evaluations the normal absorption of the Li-metal was corrected out and errors are of pure statistical nature. While the first two approaches yield the same result the third method deviates slightly. This is likely due to residual problems from applied corrections to eliminate beam energy and intensity drifts. The amount of Li clearly detected in this particular measurement was as small as 14.5 μg. The statistical error indicates that down to ten times smaller amounts could be detected. It is important to notice that the last approach does not require any spectroscopic information and might be used with a simple photon counter at very high count rates such as those that will be available from next generation laser-Compton light sources. The time stability of the ID15a monochromator was the limiting factor during this measurement

In order to demonstrate NRF-based radiography and in particular to illustrate the isotopic selectivity a sample set consisting of vials with natural LiF and isotopically

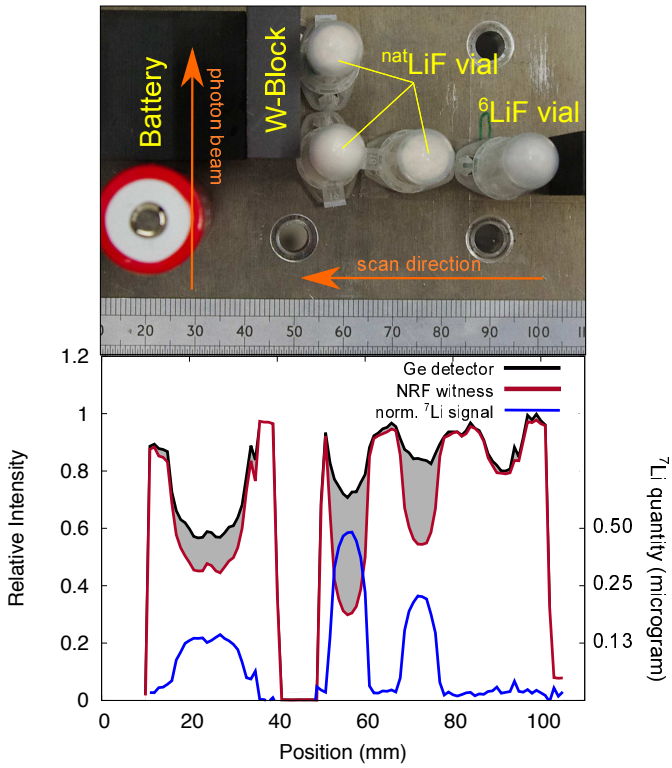

FIG. 5: Scan of a sample set consisting (from right to left) vials with isotopically enriched ^{6}LiF powder, natural LiF poweder, a tungsten block and a commercial battery. Three curves are shown: i) the intensity signal of the ID15a beam in the Ge-detector, used to illustrate a classical radiography, ii) the intensity variation of the NRF witness peak in the $LaBr_3$ detector and iii) a signal computed in regions over which there was appreciable beam transmission as ratio of the first two as a measure of the presence of ^{7}Li.

enriched ^{6}LiF powder was prepared. While an "absorption" radiography would not be able to distinguish the different isotope concentrations, NRF provides a sensitive signal. An additional two vials of natural LiF were added to illustrate the potential for obtaining quantitative information from the images. The final object to be imaged is a commercially-available, rechargeable Li-battery - UltraFire^{TM}BRC 18650. The battery contains an unknown Li-compound enclosed in a spiral metallic cathode and a metal cylinder. The battery can be used to illustrate the capability of imaging Li behind heavier elements such as stainless steel. The sample table containing all objects was scanned horizontally over 100 positions. The time stability of the monochromator was the limiting factor during this measurement. The data were evaluated according to the classical spectroscopic approach. The result is shown in Fig. 5, together with a "absorption" radiograpy based on the count rate of the Ge-detector. Obviously the "absorption" radiography does not distinguish between the two Li isotopes. In the contrary the signals of the scintillator - obtained from

spectroscopic NRF evaluation- clearly distinguish the isotopes. Comparing the measurement of a single and two vials with LiF the NRF-signal indicates good quantitative measurement of the Li-amount in the vials. The "absorption" radiograph also suggests a higher amount of material hidden in the battery (due to attenuation by the metal container and the cathode) if compared to the two LiF vials. The difference of conventional and NRF radiograph non-destructively indicates the location of the lithium material behind the metal container of the battery. The spatial resolution of the 1 dimensional image is set by the scan steps of 1 mm used in the experiment. In principle the resolution can be in the order of the beam size, i.e. about 100 μm.

In conclusion, using a novel, witness-material-based detector architecture, we have demonstrated for the first time isotope-specific, photon-based, assay and imaging of microgram-scale quantities of ^{7}Li. With this setup the detection/imaging system can be largely separated from the actual sample. The method is capable of detecting and quantifying ^{7}Li behind heavy material shielding and of distinguishing isotopic abundance.

These studies were conducted at spectral bandwidths two orders beyond the present state of the art of laser-Compton gamma-ray sources but comparable to next generation, tunable MeV gamma sources currently under development [9, 10]. The narrow-bandwidth and higher flux of the next generation machines in combination with the methods described in this study should enable non-destructive assay of shielded objects with nanogram precision and imaging with micron-scale resolution. The method is extendable to higher photon energies and fluxes and illustrates the viability of calorimetric based detection schemes based on combinations of resonant and non-resonant witness samples [18]. Such schemes do not rely upon single photon counting and are ideally matched to the high flux per pulse outputs of future laser-Compton machines. This experiment also hints at important requirements for future NRF-based detection, assay and imaging studies. For NRF-based imaging and detection of heavier isotopes and at higher photon energies (1 to 4 MeV) the signal/noise ratio becomes worse since the scattered radiation scales with the electron number. This, together with the mentioned limitations of the current experiment underlines the need for a dedicated, highly selective ($\Delta E/E \simeq 10^5$ bandwidth) and stable monochromatisation system for future NRF-based techniques. Such techniques exist [17] and were used in the past for ultra high resolution spectroscopy and when combined with future tunable γ-ray sources will enable rapid 2D and 3D isotope-specific imaging.

Support from the DFG under grant No. SFB 634 is gratefully acknowledged. This work was also performed under the auspices of the U.S. Department of Energy by Lawrence Livermore National Laboratory under Contract DE-AC52-07NA27344 The authors wish to thank Chris Ebbers, Micah Johnson and Bonnie McDonald for assistance with logistics.

[1] J. Pruet *et al.*, Journ. Appl. Phys. **99** (2006) 123102-123101-123111
[2] U. Kneissl, N. Pietralla, and A. Zilges, J. Phys. (London) **G32**, R217 (2006)
[3] S. Amano *et al.*, Nucl. Instr. Meth. A **602**, 337-341 (2008).
[4] H.R. Weller *et al.*, Mod. Phys. Lett. A **18** 23, 15691590 (2003)
[5] F. Albert *et al.*, Phys.Rev. C **13** 7, 070703 (2010)
[6] D.J. Gibson *et al.*, Phys. Rev. ST Accel. Beams 13 **7**, 070704, (2010)
[7] F. Albert *et al.*, Opt. Lett **35** 3 (2010) 354-356
[8] N. Kikuzawa *et al.*, Jap. J. Appl. Phys. **50** 10R (2011) 1347-4065
[9] C.P.J. Barty *et al.* Proceedings of the 52 Annual Meeting of the Institute for Nuclear Material Management Vol 3. 2645-2654 (2011)
[10] http://www.eli-np.ro/documents/ELI-NP-WhiteBook.pdf
[11] D. Balabanski *et al.* Journ. Phys. **590** (2015) 012005
[12] Petrillo V *et al.* Nucl. Instr. Meth. A **693** (2012) 109
[13] R. Hajima in N̈uclear Physics and Gamma-Ray Sources for Nuclear Security and Nonproliferation; World Scientific (2014) 25-31
[14] D.R. Tilley *et al.*, Nucl. Phys. A **708** (2002) 3-163
[15] http://www.esrf.eu/UsersAndScience/Experiments/StructMaterials/ID15
[16] H.T. van Dam *et al.*, IEEE Trans. Nucl. Scien. **59** 3 (2012), 656-664
[17] E. Kessler *et al.*, Nucl. Instr. Meth. A **457** 1-2 (2001) 187-202
[18] Barty, C. P. J. (2013). Dual isotope notch observer for isotope identification, assay and imaging with mono-energetic gamma-ray sources. US patent US8369480 B2, Lawrence Livermore National Security LLC